HEFAT2012
9th International Conference on Heat Transfer, Fluid Mechanics and Thermodynamics
16 – 18 July 2012
Malta

CFD AS A DESIGN TOOL FOR A CONCENTRIC HEAT EXCHANGER

J.P. Oosterhuis[1,*], S. Bühler[1], D. Wilcox[2], T.H. van der Meer[1]
*Author for correspondence
[1] Department of Thermal Engineering, University of Twente, P.O. Box 217, 7500AE, Enschede, The Netherlands, E-mail: j.p.oosterhuis@utwente.nl
[2] Bosch Thermotechnology, P.O. Box 3, 7400AA, Deventer, The Netherlands

ABSTRACT

A concentric gas-to-gas heat exchanger is designed for application as a recuperator in the domestic boiler industry. The recuperator recovers heat from the exhaust gases of a combustion process to preheat the ingoing gaseous fuel mixture resulting in increased fuel efficiency. This applied study shows the use of computational fluid dynamics (CFD) simulations as an efficient design tool for heat exchanger design. An experimental setup is developed and the simulation results are validated.

INTRODUCTION

To increase the fuel efficiency of gas-fired domestic boiler appliances, the principle of recuperation is investigated. By recovering heat from the exhaust gases of the combustion process, the ingoing fuel mixture is preheated. This preheating results in an increased adiabatic flame temperature and hence in an increase in fuel efficiency [1]. The heat transfer from the exhaust gases to the ingoing fuel mixture is usually achieved by the application of a compact gas-to-gas heat exchanger (recuperator). Implementing recuperation in practical applications was for long a niche because of high costs in relation to the gain in efficiency which made them not economically feasible [2]. However, rising energy prices and emissions legislation have changed this fact, resulting in numerous recuperator research activities being carried out in recent years.

In this study a recuperator design is proposed for a specific type of gas-fired domestic boiler appliance. Based on the results of preliminary design iterations, in combination with manufacturability and the current system lay-out, it was decided to focus on a counter-flow concentric tube heat exchanger design. In this heat exchanger type the exhaust gases flow through a tube in the center, while the fuel mixture counter-flows through the surrounding ring shown in the geometry in Figure 1. In this way the fuel mixture acts as an insulator to thermally insulate the exhaust gases from the interior of the appliance.

A common approach to design a heat exchanger is the use of a one-dimensional model such as the P-NTU, ε-NTU or LMTD method [3][4]. However, these methods do not take into account additional effects such as axial conduction and non-uniform heat transfer coefficients. Although extension of these 1D models to include such effects is generally possible, detailed temperature and velocity profiles in flow cross section cannot be obtained. In cases where this information is required to make proper design decisions, computational fluid dynamics (CFD) comes into focus as a relevant design tool.

In the recuperator design presented in this study, good flow temperature uniformity in the radial direction is of high importance in order to prevent undesired auto-ignition of the fuel mixture. Therefore a CFD model is proposed which can be used as a realistic design tool capturing detailed information about heat exchange and flow temperature uniformity.

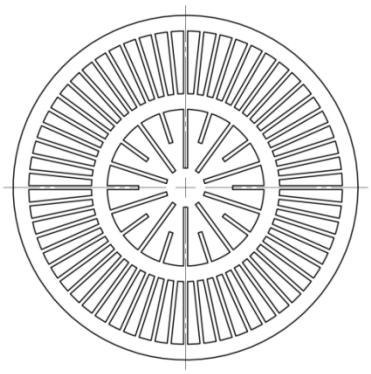

Figure 1 Core profile of designed concentric heat exchanger, $L_{core} = 200$ mm, $D_{out} = \varnothing\, 88$ mm.

NOMENCLATURE

α	[°]	Angular location around core
A_c	[m^2]	Flow cross-sectional area
C_p	[kJ/kg·K]	Specific heat capacity at constant pressure
D_h	[m]	Hydraulic diameter, $D_h = \frac{4A_c}{P}$
D_{out}	[m]	Core outside diameter
ε_{rel}	[-]	Relative solution error of numerical simulation
k	[W/m·K]	Thermal conductivity

L_{core}	[m]	Core flow length
$\dot{m}$	[kg/s]	Mass flow rate
μ	[kg/m·s]	Dynamic viscosity
N	[-]	Number of nodes or number of flow channels
$\bar{p}_{rel}$	[Pa]	Relative static pressure
p_{ref}	[Pa]	Absolute reference pressure
P	[m]	Perimeter
Re	[-]	Reynolds number, $Re = \frac{\bar{v} D_h \rho}{\mu}$
r_{eff}	[-]	Effective mesh refinement level
ρ	[kg/m^3]	Density
S	[m/s]	Absolute global flow non-uniformity
S_i	[-]	Relative local flow non-uniformity in flow channel i
T	[K]	Temperature
ΔT	[K]	Temperature difference
θ	[var]	Target variable in numerical simulation
τ	[s]	Residence time
v_i	[m/s]	Flow velocity in flow channel i
$\bar{v}$	[m/s]	Average flow velocity over flow cross-section
ξ	[-]	Scaled dimension over flow channel width
z	[m]	Axial (flow) direction

Subscripts

1	Exhaust gas domain
2	Gas/air-mixture domain
in	Location at inlet
out	Location at outlet
I	Indicates refined mesh
II	Indicates coarser mesh

DESIGN PARAMETERS

Based on the boiler appliance under investigation, a number of design parameters are defined. The exhaust gas enters the heat exchanger at $T_{1,in} = 1032\,\text{K}$ with a density of $\rho_{1,in} = 0.330\,\text{kg/m}^3$ and a specific heat capacity $C_{p\,1,in} = 1.283\,\text{kJ/kg}\cdot\text{K}$. The gas/air-mixture enters the heat exchanger in counter-flow configuration shown in Figure 2, at $T_{2,in} = 293\,\text{K}$ with a density of $\rho_{2,in} = 1.136\,\text{kg/m}^3$ and a specific heat capacity $C_{p\,2,in} = 1.055\,\text{kJ/kg}\cdot\text{K}$. The mass flow rate of both the exhaust gas and gas/air-mixture stream equals $\dot{m} = 0.001336\,\text{kg/s}$. The desired temperature increase for the gas/air-mixture $\Delta T_2 = 288 \sim 400\,\text{K}$ aims at producing the maximum increase in efficiency. Higher values are limited due to possible auto-ignition of the gas/air-mixture, which has to be prevented in order to obtain safe operation. The core flow length is fixed by the system configuration to $L_{core} = 200\,\text{mm}$ and the core material is chosen to be aluminum having a thermal conductivity of $k = 237\,\text{W/m}\cdot\text{K}$. Due to the system interfaces for the exhaust gas the headers require a 90° bend to allow for a straight recuperator core.

SIMULATION METHOD

To benefit from the (rotational) periodic geometry of the heat exchanger core compared to the heat exchanger headers, the simulation and design of core and headers has been separated. In first instance the core is designed to meet the required temperature specifications. Secondly the headers are designed based on maintaining flow uniformity to reduce the risk on hot spots and possible auto-ignition of the gas/air-mixture.

Four major assumptions are required in order to provide a fully defined simulation model. No heat transfer in the headers is assumed, i.e. the flow temperatures at the inlet and outlet of the headers equals those at the corresponding inlet and outlet of the recuperator core. Uniform outflow from the headers to the core is assumed in the recuperator core simulations and the influence of heat transfer on the flow field is neglected in the header simulations. The outer shell is assumed to be well insulated and hence heat loss through the outer core walls is neglected. All CFD simulations are performed using ANSYS CFX v13.0 with a high resolution advection scheme and a convergence criterion for momentum, mass and energy transport of $RMS \leq 1 \cdot 10^{-6}$. For a detailed description of the governing Navier-Stokes equations solved in ANSYS CFX, the reader is referred to the documentation [5].

Core Model Configuration

The core model has been subdivided into two fluid domains and one solid domain. Rotational periodicity has been applied and only 1/3 of the actual geometry is modeled. On the inlets of the fluid domains, a fixed mass flow rate is specified resulting in a uniform flow inlet velocity boundary condition. Moreover the inlet temperature is specified. On the outlets of the fluid domains an average relative static pressure boundary condition is specified of $\bar{p}_{rel} = 0\,\text{Pa}$. Reference pressure is set to $p_{ref} = 1 \cdot 10^5\,\text{Pa}$. All other boundaries of the fluid domains are specified by the interface with the solid domain inquiring a no slip wall condition and a continuous heat flux through the wall. As the expected maximum Reynolds numbers are in the range of $Re = 300 \sim 1500$, the fluid flow is modeled laminar. The boundary conditions of the solid domain are fully defined by the interface with the corresponding fluid domains and an adiabatic boundary condition on the outer walls. A schematic representation of the model configuration is shown in Figure 2.

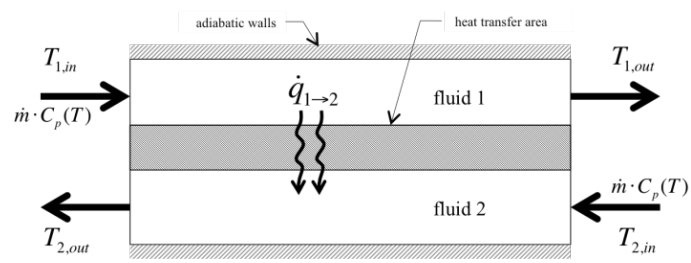

Figure 2 Outline of recuperator core model.

Header Model Configuration

Due to the relative low pressure drop in the core, the inlet and outlet header geometry influence each other's performance and must be taken into account together. As the effect of the flow field on the temperature distribution is already known from the core simulations, only cold flow simulations are used for the header design. This allows decoupling of the two different fluid domains; moreover the solid domain has become redundant. Hence a simulation model consisting of header – core – header is constructed.

Regarding the boundary conditions, the same inlet and outlet boundary conditions are used as described in the core model configuration: uniform mass flow rate at the inlet and a pressure boundary condition at the outlet. A constant fluid temperature has been specified as the average temperature of

the concerning fluid predicted by the core simulation. Along the remaining boundaries of the fluid domain, a no-slip wall condition is defined.

Due to larger hydraulic diameters in the headers, turbulent flow can be expected. In the gas/air-mixture domain the small flow channels and corresponding influence of the walls it was decided to use the SST turbulence model. In the exhaust gas domain the $k-\varepsilon$ model is used to retain robustness and numerical convergence [6].

The main goal of the header design is to preserve a uniform flow inside the heat exchanger core for optimal performance. To quantify this, a velocity-based flow non-uniformity is defined [7]:

$$S_i = \frac{v_i - \bar{v}}{\bar{v}} \tag{1}$$

$$S = \sqrt{\frac{1}{N}\sum_{i=1}^{N}(v_i - \bar{v})^2} \tag{2}$$

Equation (1) shows the relative local flow non-uniformity in flow channel i with v_i the average flow velocity in one channel and $\bar{v}$ the average flow velocity over the total cross-section. Equation (2) shows the absolute global flow non-uniformity over all flow channels. The flow non-uniformity will be calculated at $z = \frac{1}{2}L_{core}$.

Mesh Validation

A mesh validation study is shown here for the final core design. Figure 3 shows the relation between the relative error, ε_{rel} and the total number of mesh points N (nodes) with

$$\varepsilon_{rel} = \frac{|\theta_{\mathrm{I}} - \theta_{\mathrm{II}}|}{|\theta_{\mathrm{I}}|} \cdot \frac{1}{r_{\mathrm{eff}}^2 - 1} \tag{3}$$

$$r_{\mathrm{eff}} = \left(\frac{N_{\mathrm{I}}}{N_{\mathrm{II}}}\right)^{\frac{1}{3}} \tag{4}$$

where θ_{II} and θ_{I} are the values of the target variable bulk temperature on a coarse mesh and a refined mesh respectively. $T_{2,out}$ and $T_{1,out}$ in Figure 3 represent the relative error in bulk temperature at the outlet of the gas/air-mixture domain and exhaust gas domain respectively. The solid lines show the maximum error in bulk temperature over the corresponding fluid domain.

From the strong decay in Figure 3 it is clear that the gas/air-mixture domain is most sensible to mesh refinement thus a second mesh study of a single flow channel has been performed using a simplified linear temperature profile as a boundary condition for the inner wall. Five meshes with an increasing number of nodes over the width of the channel (ξ-direction) are investigated: 4, 6, 9, 12 and 31 nodes. The mesh with 4 nodes corresponds to the mesh with the highest number of nodes shown in Figure 3. The temperature profile in the ξ-direction at the outlet of the channel is shown in Figure 4. The mesh with 31 nodes in the ξ-direction results in a close to quadratic temperature profile. It is observed that after a short entrance length of $z = 0.05 \cdot L_{core}$, this quadratic profile is obtained and hence the flow is considered thermally fully developed. This quadratic velocity and temperature profile is already well defined with only 6 nodes and no significant deviations are observed. This result highly reduces computational costs. Applying this mesh resolution to the total core mesh results in a mesh with $3.90 \cdot 10^6$ nodes.

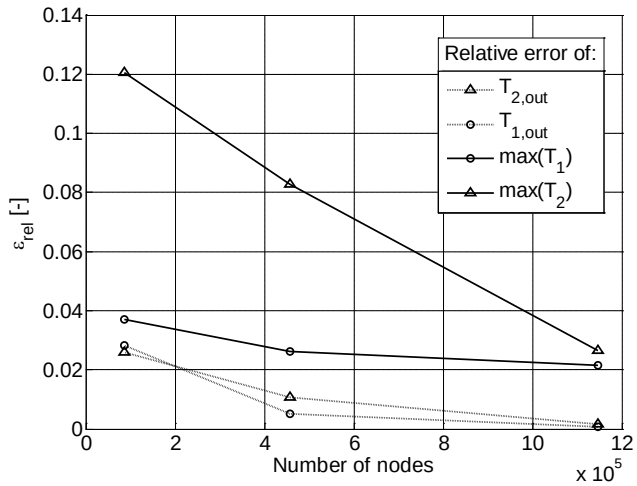

Figure 3 Relative error in bulk temperature compared for different mesh sizes.

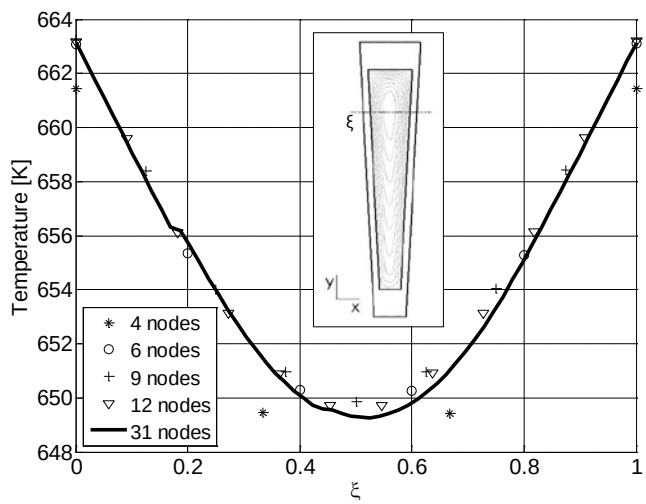

Figure 4 Temperature profile at outlet of single channel for various mesh sizes; insert shows location of profile on outlet.

SIMULATION RESULTS

Various core designs have been designed and their performance has been investigated using the aforementioned simulation model. Due to the predefined simulation setup, changing the design and setting up a new simulation was reduced to only a couple of hours. Different design changes mainly affect the number of fins and their geometry in both fluid domains. The first concentric design shows a temperature increase in the gas/air-mixture of $\Delta T_2 = 279\,\mathrm{K}$ while the cross-sectional temperature gradient at the outlet is $237\,\mathrm{K}$. After 7 design iterations this gradient is reduced to only $14\,\mathrm{K}$, while

$\Delta T_2 = 372\,\mathrm{K}$ is close to the desired maximum of $400\,\mathrm{K}$. The simulation results are summarized in Table 1.

	Exhaust gas	Gas/air-mixture
Bulk velocity v_{bulk}	2.9 m/s	0.43 m/s
Residence time τ	0.069 s	0.47 s
$\max(Re)$	1077	
$\max(\Delta P)$	8.1 Pa	
Overall heat transfer $\dot{Q}$	567 W	

Table 1 Summary of core simulation results.

The final core design is shown in Figure 1. Sixty axial fins are used in the gas/air-mixture domain; in the exhaust gas domain 20 axial fins with alternating length are used. The simulated axial bulk temperature profile is presented in Figure 5. Note the very smooth temperature increase of the gas/air-mixture as it approaches the solid temperature. Due to the fixed flow length and large difference between exhaust gas temperature and maximum allowable gas/air-mixture temperature, this "inefficient" heat exchanger design is necessary to obtain the required temperature uniformity in the gas/air-mixture to avoid hot spots.

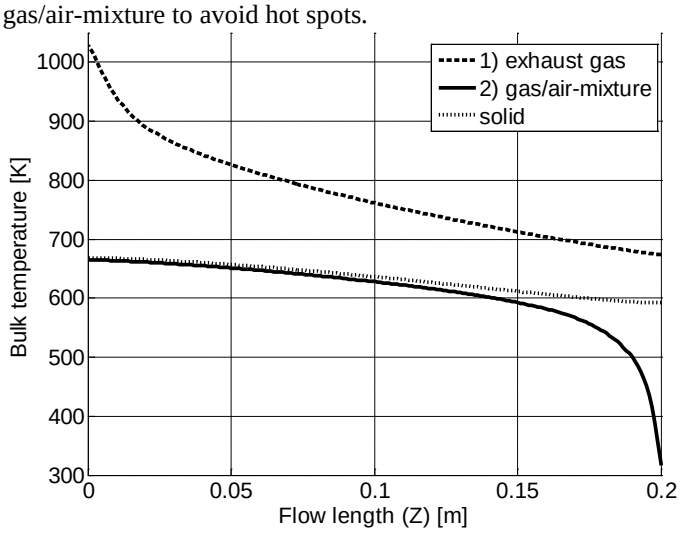

Figure 5 Simulated bulk temperature profile in axial direction of heat exchanger core; exhaust gas inlet at $z = 0$, gas/air-mixture inlet at $z = 0.2$.

Header Design and Simulation Results

One major difference between the designs of the two different fluid domains is of large influence on the different header configurations: the gas/air-mixture domain consists of 60 separated flow channels while the exhaust gas domain is only one physical flow channel. To avoid back-flow, the distribution of the flow over the 60 channels is critical and therefore the focus is on designing a well performing gas/air-mixture header, while the exhaust gas header is designed secondarily.

By using the simulation model with decoupled fluid domains, a number of quick design iterations for the gas/air-mixture headers are performed. From an initial gas/air-mixture header design with an absolute global flow non-uniformity of $S = 1.22\,\mathrm{m/s}$ (284 % of the bulk velocity), the flow non-uniformity is reduced to $S = 0.038\,\mathrm{m/s}$ (8.8 % of the bulk velocity) in 8 design iterations with various inlet and outlet header combinations. This final design (integrated with the exhaust header design) consisting of an equal inlet and outlet header is shown in Figure 6. In Figure 7 the relative local flow non-uniformity for the final design is shown as a function of the angular location in the core. The obstruction of the exhaust gas header in the gas/air-mixture header results in a lower relative velocity at that particular location (around $\alpha = 180°$).

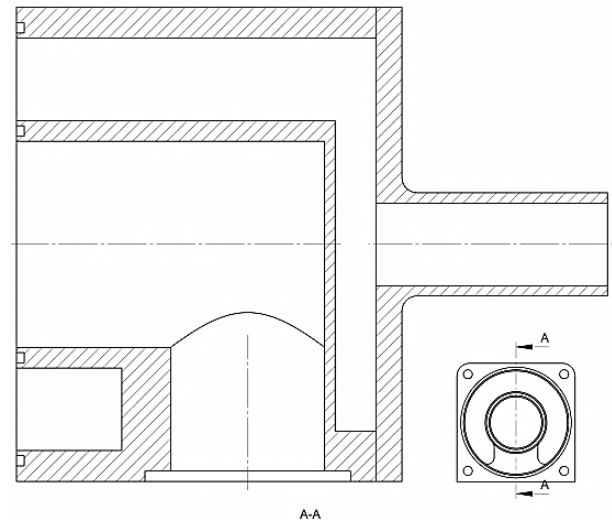

Figure 6 Integrated header design for both inlet and outlet header.

From a system integration point of view, the design of the exhaust gas header requires 90° bend on both the inlet and outlet header. A bent design with a constant diameter equal to the core inside diameter showed low flow non-uniformity: $S = 0.43\,\mathrm{m/s}$ (15 % of the bulk velocity), thus no further optimization is performed. In Figure 8 the relative local flow non-uniformity for the exhaust gas header is shown. The bent design results in a slightly accelerated flow at the $\alpha = 0°$.

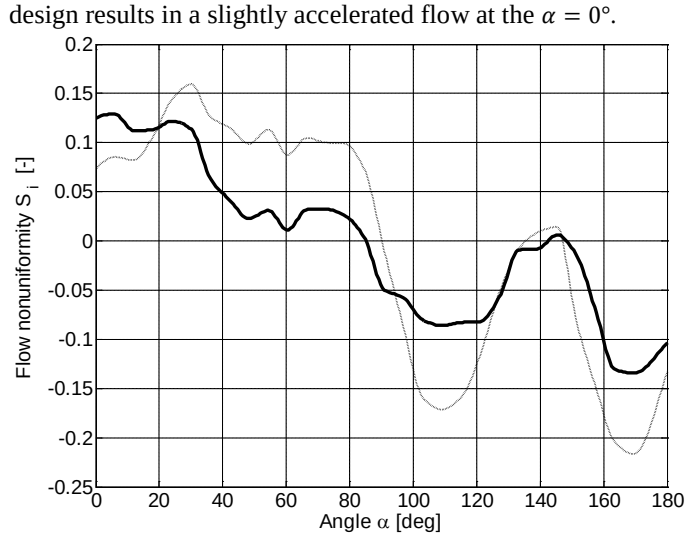

Figure 7 Relative local flow non-uniformity S_i for gas/air-mixture header; both minimum mass flow rate (solid line) and maximum mass flow rate (dashed line) are shown.

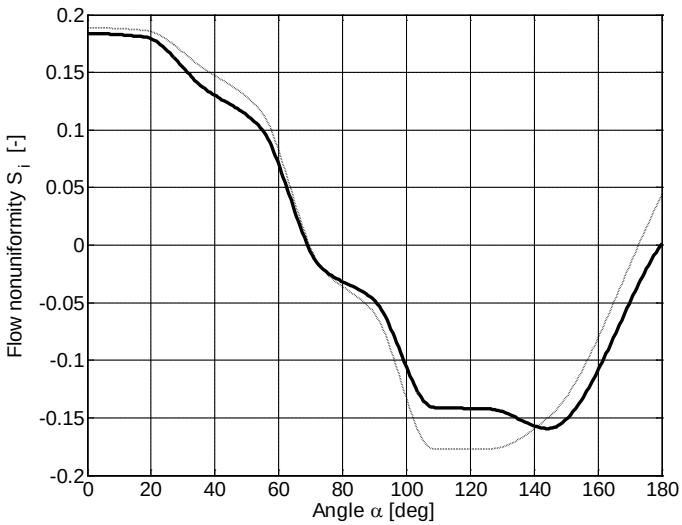

Figure 8 Relative local flow non-uniformity S_i for exhaust gas header; both minimum mass flow rate (solid line) and maximum mass flow rate (dashed line) are shown.

EXPERIMENTAL METHOD

To validate the simulation results of the recuperator core and headers, an experimental setup has been built. Using this setup, boundary conditions regarding inlet temperature and velocity can be imposed on the recuperator prototype. A schematic overview of this setup is shown in Figure 9. The black dots indicate locations where temperature is measured; the two black squares indicate the velocity sensors. Two velocity sensors with a measurement accuracy of ±2.0% are used to control both fans to obtain the desired mass flow rate.

For safety reasons ambient air is used as the test fluid instead of exhaust gas and a gas/air-mixture. The hot fluid is heated by an electric flow-through heater up to $T_{in} = 673\,\mathrm{K}$. Note that this is lower than the actual exhaust gas inlet temperature but for validation purposes the simulations have been adjusted to the measured inlet temperature and velocity as well as the changed gas composition.

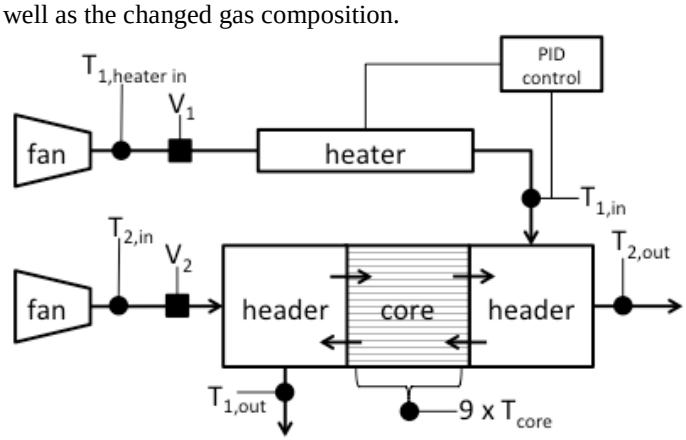

Figure 9 Schematic of experimental validation setup.

Thermocouples with a measurement accuracy of ±1.5 K are located at both inlets and outlets as well as at nine locations within the core outer flow channels: at 3 locations in axial direction ($z = 37, 87, 137\,\mathrm{mm}$) and at 3 different angular locations around the core. Thermocouples with a small diameter of 0.25 mm, to minimize flow disturbance, are mounted and centered in the flow channels. As soon as a steady operation point is reached, the temperature is measured and averaged over an interval of 60 s.

EXPERIMENTAL RESULTS

Using the previously described experimental method, the simulation results have been validated using a hot gas inlet temperature of $T_{in} = 673\,\mathrm{K}$. The core simulation has been carried out again with adjusted inlet parameters (temperature and mass flow rate). The axial bulk temperature profile is compared with measured values in Figure 10. Along the core the deviation in temperature is small, but at the exit of the cold air flow (representing the gas/air-mixture) the measured temperature is about 15 K higher than the simulated temperature. This is caused by heat exchange in the headers which was not taken into account in the simulation model. This effect cancels the effect of heat loss from the core to the environment on the measured temperatures. The interaction between heat exchange in the headers and heat loss to the environment on the measured bulk temperatures is confirmed by carrying out the same experiment with lower inlet temperatures ($T_{in} = 373, 473, 573\,\mathrm{K}$). This shows a relative higher heat loss from the core as the influence of heat exchange in the headers is smaller.

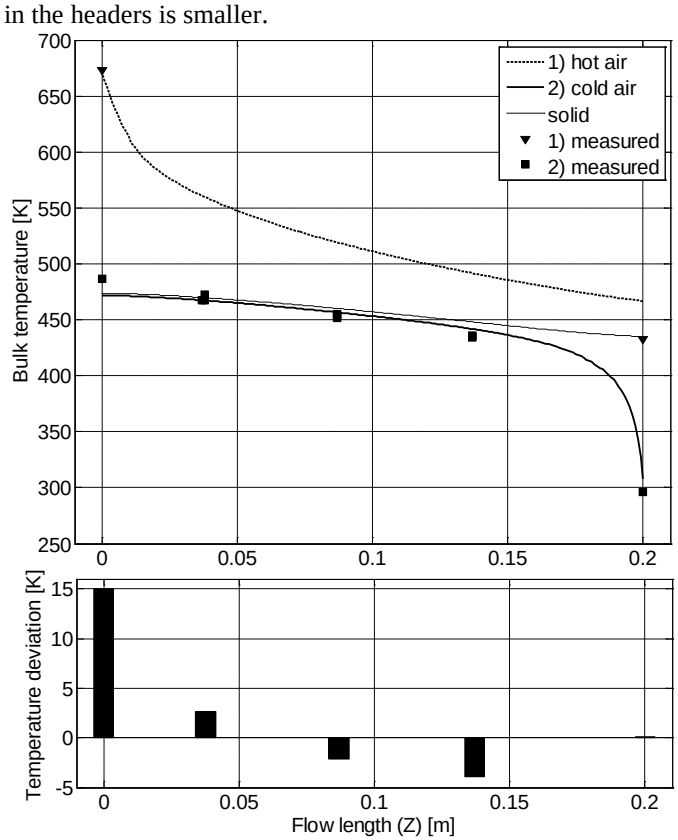

Figure 10 Bulk temperature profile of core simulation (lines) compared with measured temperatures (dots); bars indicate difference in temperature of gas/air-mixture.

By measuring the radial temperature profile in a single flow channel using a hot flow inlet temperature of $T_{in} = 673\,\mathrm{K}$, the effect of the assumed adiabatic walls becomes more visible. In Figure 11 the simulated radial temperature profile is compared with a polynomial fit through measured values at several radial locations. Although the mean deviation is small, a clear difference in shape is visible closer to the outer wall. The simulation predicts a local increase in temperature due to the adiabatic walls whereas this effect is totally absent in the experimental situation.

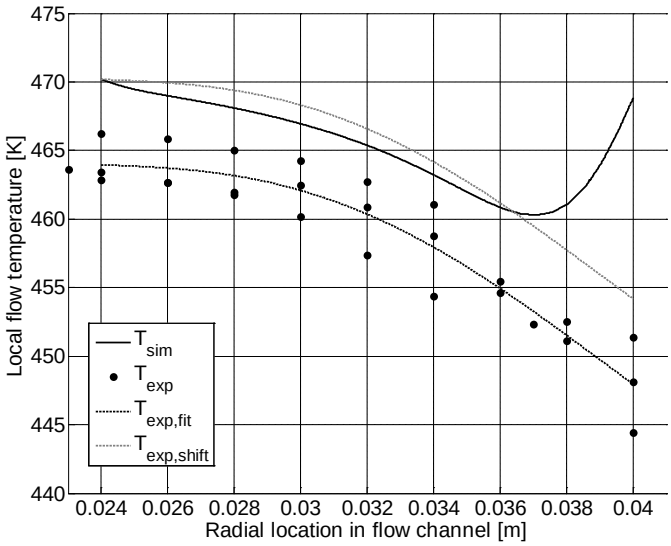

Figure 11 Radial temperature profile in core channel at $z = 37$ mm; solid line represents simulation results, black dashed line is fit through experimental results (dots).

By rotating the recuperator core with respect to the headers, the angular temperature profile is measured. Based on the simulated flow non-uniformity due to the headers, a certain amount of temperature non-uniformity in the angular direction is expected. However, the temperature difference in the angular direction is within the range of $10\,\mathrm{K}$ and as such smaller than the radial temperature gradient. It is likely that the high conductivity of the aluminum used causes a uniform cross-sectional temperature distribution in the core material which at least eliminates the effect of the flow non-uniformity in the hot air supply stream.

CONCLUSION

For heat exchanger design cases where one dimensional models are not sufficient, CFD should be considered as a relevant design tool. By applying a number of assumptions; i.e. no heat transfer in the headers, uniform inflow in the core and neglecting influence of heat transfer on the flow field; the design of headers and core can be separated. Moreover, the headers can be designed for each fluid flow separately. A mesh validation study shows that a relatively coarse mesh provides accurate and relevant results. This allows for quick and efficient design iterations, resulting in a recuperator concept that meets all design requirements.

Using CFD simulations a concentric heat exchanger core is designed to provide up to $567\,\mathrm{W}$ of recuperation in a domestic boiler appliance. Obtaining the desired amount of heat transfer within the constraint flow length is achieved by 20 axial fins in the exhaust gas flow. In the gas/air-mixture flow 60 axial fins are used both to enhance heat transfer and to avoid high temperature gradients over the cross-section.

To design the headers, CFD simulations under cold flow conditions are carried out to compute the flow field and resulting flow non-uniformity. Using an inflow and outflow configuration for the gas/air-mixture that is normal to the core flow direction a small flow non-uniformity is obtained. On the exhaust gas side, a bent inlet and outlet is used to prevent interference with the gas/air-mixture stream.

Experimental validation of the simulation work does clearly reflect the assumptions performed in the simulations. Although heat loss from the recuperator core to the environment and additional heat transfer in the headers balance each other using a hot flow inlet temperature of $T_{in} = 673\,\mathrm{K}$, at lower inlet temperatures these two effects can be clearly distinguished. However, absolute deviation of measured temperatures from simulated values is not larger than $20\,\mathrm{K}$, which is considered as good correspondence compared to the high operation temperatures. Influence of flow non-uniformity caused by the headers is not visible in the temperature field inside the recuperator core as a consequence of the high thermal conductivity.

Hence the use of CFD simulations as a quick design tool for gas-to-gas heat exchanger design shows good correspondence with experimental results. Neglecting heat loss and separating core and header design only leads to small deviations whilst highly reducing the computational resources. Applying the proposed design approach reduces the need of prototypes hence saving time and costs.

ACKNOWLEDGEMENTS

This research has been carried out as part of a master thesis in Mechanical Engineering at the University of Twente, The Netherlands. As the recuperator is intended to be part of a domestic boiler appliance, all experimental work has been carried out in co-operation with Bosch Thermotechnology. Computational resources and software were provided by the University of Twente.

REFERENCES

[1] S. R. Turns, *An introduction to combustion*. New York: McGraw-Hill, 2000.
[2] J. E. Hesselgreaves, *Compact heat exchangers: selection, design, and operation*. Pergamon, 2001.
[3] W. Kays and A. London, *Compact heat exchangers*, Third. Malabar, Florida: Krieger Publishing Company, 1998.
[4] R. K. Shah and D. P. Sekulić, *Fundamentals of heat exchanger design*. Hoboken, New Jersey: John Wiley & Sons, Inc., 2003.
[5] ANSYS, *ANSYS CFX Reference Guide*. 2009.
[6] ANSYS, *ANSYS CFX-Solver Modeling Guide*. 2009.
[7] J. Wen and Y. Li, "Study of flow distribution and its improvement on the header of plate-fin heat exchanger," *Cryogenics*, vol. 44, no. 11, pp. 823-831, Nov. 2004.